Radiation Physics and Chemistry 166 (2020) 108517

Contents lists available at ScienceDirect

Radiation Physics and Chemistry

journal homepage: www.elsevier.com/locate/radphyschem

Evaluation of gamma attenuation parameters and kerma coefficients of YBaCuO and BiPbSrCaCuO superconductors using EGS4 code

Hasan Baltas

Recep Tayyip Erdogan University, Department of Physics, 53100, Rize, Turkey

ARTICLE INFO

Keywords:
Superconductors
γ-Kerma coefficient
EGS4 code
Attenuation coefficient.

ABSTRACT

The levels of the coefficients of the mass attenuation (μ/ρ) for YBaCuO and BiPbSrCaCuO superconductors and their contents were determined theoretically, using EGS4 simulation code and the XCOM database, and experimentally at gamma-ray energies of 511, 661 and 1274 keV. Additionally, radiation attenuation parameters such as half value layer (HVL), mean free path (MFP) and effective atomic number (Z_{eff}) for investigated superconductors samples were calculated using the obtained μ/ρ values. It was observed that the theoretical and the experimental values were in agreement. Furthermore, the gamma-ray kerma coefficient k of these elements and superconductor samples was evaluated theoretically and experimentally, based on results of the mass attenuation coefficients determined at the same energies, and good agreement was observed. The theoretical levels of these coefficients were also computed over an expanded energy interval from 1 keV to 100 MeV using the WinXCom program. The results show that the calculated gamma kerma coefficient values of BiPbSrCaCuO had the highest atomic number, which was higher than for the YBaCuO superconductor.

1. Introduction

Superconductors are utilized in science, research and technological advancement, as well as in implementations in medicine. The biggest application for superconductivity is in the high-intensity magnetic fields required for MRI and NMR. One other significant area of the implementation of superconductors involves superconducting electronics, such as superconducting quantum interferometer devices and radiation sensors (Luiz, 2011). In the future, superconductors are expected to be used for magnets in nuclear fusion reactors or accelerators, and these materials may be exposed to radiation (Ueda et al., 2009). It is important to know the effects of radiation on the operating characteristics of the magnets. Thus, it is clearly of interest to study the effects of radiation on the properties of superconductors. Radiation attenuation parameters such as mass attenuation coefficient, effective atomic number, half value layer and mean free path are highly important for not only applied but also theoretical sciences, and they are beneficial for several applied areas like nuclear diagnostics, protection against radiation, nuclear medicine and radiation dosimetry (Baltaş et al., 2007). A software called XCOM was created by Berger and Hubbell (1987), and this software computes attenuation coefficients and photon cross sections for elements, compounds and mixtures in an energy interval from 1 keV to 100 GeV. Gerward et al., 2001 modified this software into a platform for windows known as WinXCOM. A Monte Carlo method was employed to compare the mass attenuation coefficient levels to experimental results to solve problems in many fields including nuclear physics, nuclear engineering, medical physics, radiation safety management and reactor design (Yamaguchi and Ohba, 2014; Tekin et al., 2017).

Gamma energy is sent to charged particles in the material via different gamma interactions such as the photoelectric effect, Compton scattering and pair production. These secondary charged particles' energy is transferred to the material by means of atomic excitation and ionisations. Thus, an amount of energy is deposited in the material as kinetic energy. The *kerma* coefficient, *K,* is an abbreviation of "kinetic energy released in materials," and this substitutes the conventional exposure as the variable of shielding design (Turner, 2008). Kerma is numerically identical to the absorbed dose at lower gamma energy. Kerma is greater than the absorbed dose, since some very energetic secondary electrons and X-rays get away from the area of interest before transferring their energy in higher-energy photons. The energy of this escape is accounted for in kerma, but not in the dose that is absorbed. In low-energy gamma-rays, this distinction is generally a negligible one. To associate the radiation going across a unit volume of a substance of concern (fluence, Φ) with the energy release (K) in the substance, the term "kerma coefficient (k)" (k; kerma per fluence, $Gy.m^2$) is commonly utilized (El-Khayatt and Vega-Carrillo, 2015; Zhang and Abdou, 1997).

E-mail address: hasan.baltas@erdogan.edu.tr.

https://doi.org/10.1016/j.radphyschem.2019.108517
Received 25 August 2019; Received in revised form 23 September 2019; Accepted 4 October 2019
Available online 08 October 2019
0969-806X/

A number of investigations have been carried out on the attenuation coefficients and on the effects of irradiation in superconductor materials (Sawh et al., 2000; Petrean et al., 2000; Krusin-Elbaum et al., 1994; Ballarino et al., 2004). Recently, several authors have calculated extensive gamma kerma coefficients for a set of composite substances like biologically important materials, alloys, compounds, gamma and neutron shielding materials, concretes, polymer dosimeters and glasses (Kondo et al., 2008; Singh et al., 2015; El-Khayatt and Vega-Carrillo, 2015; El-Khayatt, 2017; Olukotun et al., 2018).

However, there are no investigations in the literature on determining gamma kerma coefficients for superconductors under exposure to gamma rays, and these are required for answering different issues in radiation physics and radiation dosimetry. Hence, this study adopted the coefficients of mass attenuation in the studied superconductors and their compounds from the study by Baltaş et al. (2005) and, half value layers, mean free paths, effective atomic numbers and kerma coefficients were theoretically calculated using the EGS4 code and the XCOM program, and also experimentally determined. These coefficients in YBaCuO and BiPbSrCaCuO superconductors and their components in different gamma energies in radiation environments were determined, and the results were evaluated.

2. Material and methods

2.1. Experimental

$YBa_2Cu_3O_7$ and $Bi_{1.84}Pb_{0.}34Sr_{1.91}Ca2_{.03}Cu_{3.06}O_{10}$ superconductor samples were prepared utilizing a solid-state reaction method. The mass attenuation coefficients of $YBa_2Cu_3O_7$ and $Bi_{1.84}Pb_{0.}34Sr_{1.91}Ca2_{.03}Cu_{3.06}O_{10}$ superconductors and their components were determined using a NaI (Tl) detector at energies of 511, 661 and 1274 keV. The density of YBaCuO and BiPbSrCaCuO samples changes from 5.12 to 5.43 g/cm^3 and 4.52 to 5.23 g/cm^3, respectively (Cevik and Baltaş, 2007). Detailed information about the computation of the experimental mass attenuation coefficients was reported in previous studies (Baltas et al., 2005).

2.2. Simulation

Simulation was conducted by using the software package EGS4 (Electron Gamma Shower Version4) (Nelson et al., 1985), which performs Monte Carlo simulations of electron-photon showers in random materials. Within the EGS4 code, a MORTRAN code applying a cylindrical model was utilized. This procedure included the arbitrary creation of emission points within the source. A RANLUX random number generator was employed with the EGS4 code, as it was demonstrated to provide superior distribution and an extended sequence (Gasparro et al., 2008).

In the model implemented alongside EGS4, the efficiency was separated into 10010 energy bins, each with a width of 0.3 keV. The particular number of bins was selected to ensure that a few bins greater than the level of highest energy were utilized to search for rounding errors in the computations.

The energy levels used for the model of simulation were ensured to turn out as 10 eV smaller than an integer to prevent energy lying at the end of a bin, since it results in rounding errors causing a non-negligible set of circumstances quantified in the next channel.

In the Monte Carlo calculations, the calculation geometry was planned for an NaI detector. As demonstrated in Fig. 1, the computed area is split into 235 cells, and when this figure is rotated over the z-axis by 360°, a cylindrical geometry is reached. Fig. 1 would therefore be considered to show a set of cylindrical annular shells, each with a radius represented with R1, R2, …, R12 and planes represented with P1, P2, …, P18. A part of code was created for the point radioactive source in a manner where all photons were released over the z-axis, giving a beam of collimated photons (Celik and Cevik, 2010; Çelik et al., 2018). In order to minimise the statistical uncertainties, sample thicknesses were selected to meet the condition $2 \leq \ln(I_0/I) \leq 4$ and 10^7 photon tracking was performed in the simulations. Calculations were performed for gamma photons of energies 511, 661 and 1274 keV. The simulated values have a relative error of less than 1%.

2.3. Radiation parameters

If a material of thickness x is placed in the path of a beam of gamma radiations, the intensity of the beam will be attenuated according to Beer-Lambert's law:

$$I = I_0 e^{-\mu x} \tag{1}$$

where I_0 and I are the unattenuated and attenuated photon intensities, respectively, and μ (cm^{-1}) is the linear attenuation coefficient of the material.

A coefficient more accurately characterizing a given material is the density-independent mass attenuation coefficient μ/ρ (cm^2/g):

$$I = I_0 e^{-(\mu/\rho)\rho x} = I_0 e^{-(\mu/\rho)d} \tag{2}$$

where d is the mass per unit area (g/cm^2). The mass attenuation coefficient, μ/ρ for a compound or a mixture is given by

$$\mu/\rho = \sum_i w_i (\mu/\rho)_i \tag{3}$$

where ρ is the density of mass of the sample, while w_i and $(\mu/\rho)_i$ are the weight fraction and mass attenuation coefficient values of the ith constituent element in sample, respectively (Kumar et al., 2019).

For a chemical compound the fraction by weight is given by

$$w_i = \frac{a_i A_i}{\sum a_i A_i} \tag{4}$$

where A_i is the atomic weight of the ith element and a_i is the number of formula units. Hence the linear attenuation coefficients are given by

$$\mu = \sum_i \rho_i (\mu/\rho)_i \tag{5}$$

where ρ_i is the partial density, i.e. the density as it appears in the mixture, of the ith constituent. Theoretical values for the mass attenuation coefficients (μ/ρ) of the superconductor specimens have been calculated by means of the WinXCom software and EGS code (Gerward et al., 2001, 2004; Celik and Cevik, 2010).

The term of Z_{eff} is a factor used to prediction of the shielding performance for any material. The Z_{eff} indicates the fraction of total number of electrons in an environment participates in photon-atom interaction number (Tekin et al., 2019). From the mass attenuation coefficient values, the effective atomic number (Z_{eff}) for the present agents has been calculated with the help of the following equation:

$$Z_{eff} = \frac{\sum_i f_i A_i (\mu/\rho)_i}{\sum_i f_i A_i / Z_i (\mu/\rho)_i} \tag{6}$$

where f_i, A_i, and Z_i represent the fractional abundance, the atomic weight, and the atomic number of the element ith, respectively (Obaid et al., 2018).

The mean free path (MFP) is the average distance between two successive collisions of photons and half value thickness (HVT) is the thickness that reduces the intensity of photons by half of its initial intensity, were calculated using μ values from the following relations (Gaikwad et al., 2019):

$$\mathrm{MFP} = \frac{1}{\mu} \tag{7}$$

$$\mathrm{HVT} = \frac{0.693}{\mu} \tag{8}$$

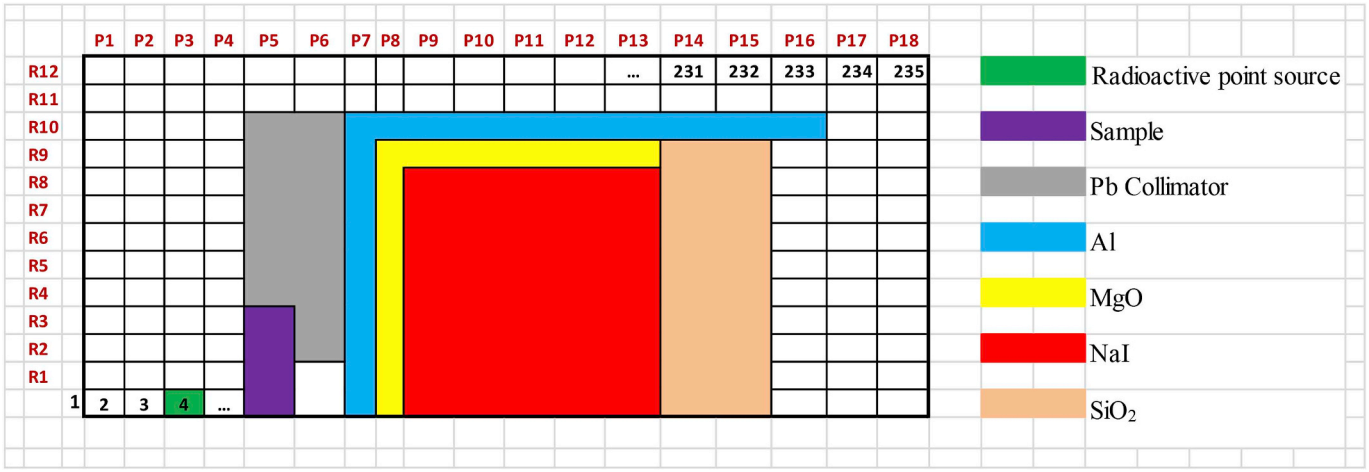

Fig. 1. Detector model for Monte Carlo (ESG4 code) calculations.

Table 1
Chemical composition (weight fraction %) of YBaCuO and BiPbSrCaCuO superconductor samples.

Compound	O	Ca	Cu	Sr	Y	Ba	Pb	Bi
$YBa_2Cu_3O_7$	16.81		28.62		13.35	41.23		
$Bi_{1.84}Pb_{0.34}Sr_{1.91}Ca_{2.03}Cu_{3.06}O_{10}$	15.12	7.68	18.38	15.82			6.65	36.34

2.4. Calculation of kerma coefficient (k)

For uncharged particles, the kerma coefficient k (in Gy.cm^2/photon) can be determined by using the coefficient of mass attenuation and the probabilities of partial interaction based on the equations below:

$$K = k\varphi\left[\frac{\mu_{tr}}{\rho}\right] \tag{9}$$

where K is uncharged radiation of energy E, $k\varphi$ is the kerma coefficient and μ_{tr}/ρ is the mass energy-transfer coefficient of the substance (Thomas, 2012).

$$k_{Ex}(E) = k_D \sum_i w^i \left[(\mu_{tr}/\rho)^i_{\tau,Ex} E + \bar{f}_C (\mu_{tr}/\rho)^i_{C,Ex} E + (\mu_{tr}/\rho)^i_{\kappa,Ex}(E - 1.022) \right] \tag{10}$$

$$k_t(E) = k_D \sum_i w^i \left[(\mu_{tr}/\rho)^i_{\tau,t} E + \bar{f}_C (\mu_{tr}/\rho)^i_{C,t} E + (\mu_{tr}/\rho)^i_{\kappa,t}(E - 1.022) \right] \tag{11}$$

where $k(E)$ is the gamma kerma coefficient at the energy level of E as experimental and theoretical, and $(\mu_{tr}/\rho)_\tau{}^i$, $(\mu_{tr}/\rho)_C{}^i$ and $(\mu_{tr}/\rho)_K{}^i$ are the photoelectric, compton scattering and pair production mass attenuation coefficients of the ith component at the gamma energy level of E, respectively. $k_D (k_D = 1.602 \times 10^{-10} Gy.\, g/MeV)$ is the coefficient of energy conversion between MeV and Gy.g. $\bar{f}_C$ is the mean fraction of the photon energy that is transmitted to the charged particles' kinetic energy created or emitted in the absorber along the Compton procedure (Attix, 1986). $\bar{f}_C$ may be predicted based on the proportion of the energy transfer, σ_{tr}, and the Compton, σ_C, cross-sections (Abdel-Rahman and Podgorsak, 2010).

$$\bar{f}_C = \sigma_{tr}/\sigma_C. \tag{12}$$

In this study, we compute $\bar{f}_C$ for superconductor specimens at photon energies of between 10 keV and 1GeV, in the sense reported by Attix (1986).

Table 2
Theoretical, calculated and experimental values of mass attenuation coefficients μ/ρ (cm^2/g).

Elements and compounds	μ/ρ (cm^2/g)								
	511 keV			661 keV			1274 keV		
	XCOM	EGS4	EX[a]	XCOM	EGS4	EX[a]	XCOM	EGS4	EX[a]
^{8}O	0.0865	0.0879	0.0860	0.0773	0.0776	0.0770	0.0564	0.0567	0.05060
^{20}Ca	0.0876	0.0865	0.0883 ± 2.2E-3	0.0779	0.0770	0.0792 ± 1.9E-3	0.0565	0.0564	0.0582 ± 1.3E-3
^{29}Cu	0.0827	0.0826	0.0824 ± 2.5E-3	0.0726	0.0719	0.0712 ± 1.8E-3	0.0521	0.0520	0.0527 ± 1.2E-3
^{38}Sr	0.0833	0.0819	0.0841 ± 2.1E-3	0.0716	0.0708	0.0723 ± 1.8E-3	0.0502	0.0500	0.0512 ± 1.3E-3
^{39}Y	0.0849	0.0848	0.0839 ± 1.6E-3	0.0728	0.0726	0.0742 ± 1.4E-3	0.0509	0.0509	0.0530 ± 1.3E-3
^{56}Ba	0.0972	0.0967	0.0991 ± 2.7E-3	0.0777	0.0773	0.0699 ± 1.7E-3	0.0500	0.0499	0.0529 ± 1.1E-3
^{82}Pb	0.1565	0.1550	0.1507 ± 2.2E-3	0.1103	0.1092	0.1085 ± 2.2E-3	0.0579	0.0578	0.0571 ± 1.3E-3
^{83}Bi	0.1602	0.1588	0.1615 ± 3.0E-3	0.1127	0.1100	0.1212 ± 3.0E-3	0.0587	0.0588	0.0557 ± 1.2E-3
$YBa_2Cu_3O_7$	0.0896	0.0891	0.0953 ± 1.8E-3	0.0755	0.0749	0.0729 ± 1.7E-3	0.0518	0.0516	0.0532 ± 1.0E-3
$Bi_{1.84}Pb_{0.34}Sr_{1.91}Ca_{2.03}Cu_{3.06}O_{10}$	0.1168	0.1154	0.1202 ± 2.4E-3	0.0907	0.0898	0.0891 ± 2.2E-3	0.0556	0.0554	0.0559 ± 1.1E-3

[a] Baltaş et al. (2005).

Table 3
The values of half value layer (HVL), mean free path (MFP) and effective atomic number (Z_{eff}) for YBaCuO and BiPbSrCaCuO superconductor.

	Energy (keV)	YBaCuO			BiPbSrCaCuO		
		XCOM	EGS4	EX	XCOM	EGS4	EX
HVL	511	1.515	1.518	1.419	1.141	1.154	1.108
	661	1.792	1.806	1.855	1.469	1.484	1.495
	1274	2.611	2.622	2.543	2.396	2.405	2.384
MFP	511	2.185	2.191	2.048	1.646	1.666	1.599
	661	2.598	2.606	2.678	2.120	2.141	2.158
	1274	3.773	3.783	3.669	3.458	3.471	3.440
Z_{eff}	511	24.79	24.45	24.70[a]	32.76	31.54	32.85[a]
	661	23.60	23.81	23.91[a]	29.11	28.95	30.07[a]
	1274	23.56	23.05	23.53[a]	27.06	26.08	26.80[a]

[a] Baltaş et al. (2005).

3. Results and discussion

The chemical compositions of YBaCuO and BiPbSrCaCuO superconductors are given in Table 1. Table 2 gives the mass attenuation coefficients (μ/ρ) in YBaCuO and BiPbSrCaCuO superconductors and their constituents determined by Monte Carlo simulation (EGS4), the XCOM program and experiment (EX) to calculate the gamma kerma coefficients. It is observed that there is satisfactory agreement between them. The levels of μ/ρ determined by XCOM in every investigated sample were found to be very close to the results of the EGS4 code at photon energies of 511, 661 and 1274 keV. The EGS4 simulation results are also found to agree well with the experimental results.

The theoretical (XCOM and EGS4 code) and the experimental values of HVL and MFP for YBaCuO and BiPbSrCaCuO superconductors are listed at the selected gamma energies in Table 3. In addition, these parameters for YBaCuO and BiPbSrCaCuO superconductor samples were theoretically calculated from the XCOM program in the energy range of 1–100 MeV, and plotted with the results of EGS4 code and the experimental data in Fig. 2 (a, b). From Fig. 2, it can be seen that the values of HVL and MFP increase with increasing photon energy for the superconductors. In addition, Fig. 2 (a) shows that BiPbSrCaCuO superconductor sample has lower HVL and MFP values thus better attenuation properties than YBaCuO superconductor sample in the low and intermediate energies. For the superconducting samples, lower HVL and MFP values indicate that the material under investigation has higher photon protection properties (Tekin et al., 2019).

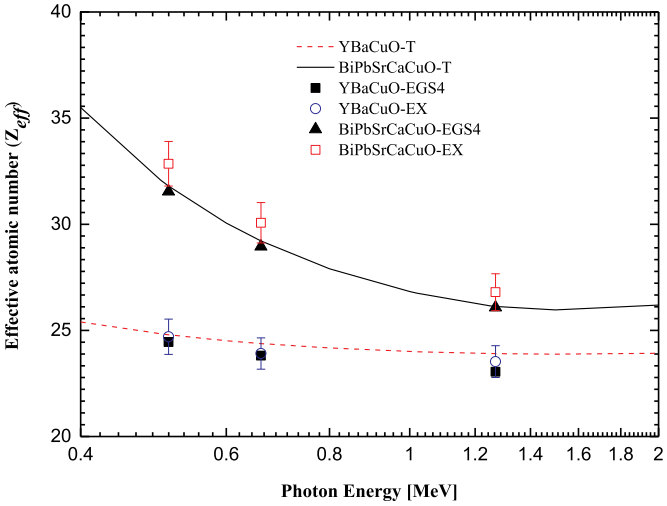

Fig. 3. Theoretical (T, EGS4) and experimental (EX) values of the effective atomic number of YBaCuO and BiPbSrCaCuO superconductor samples at different energies.

By using the theoretical (EGS4 code and XCOM data) and the experimental data of μ/ρ, the effective atomic numbers (Z_{eff}) for YBaCuO and BiPbSrCaCuO samples were determined and listed in Table 3. Fig. 3 displays a plot of Z_{eff} against gamma energy for the studied superconductor samples. As clearly seen from the figure that Z_{eff} decreases with increasing energy. It is obvious that the Z_{eff} values of BiPbSrCaCuO are higher than YBaCuO. This different in Z_{eff} depends on the spread in the high atomic numbers of which the material is composed.

The (μ/ρ) values were then utilized to compute the gamma kerma coefficients using Eq. (10) and (11). The theoretical (K_T), simulation (K_{EGS4}) and experimental (K_{Ex}) values of the gamma kerma coefficients for the superconductors and the six elements are given in Table 4 for energies of 511, 661 and 1274 keV. From this table, it can be seen that the EGS4 simulation results for the gamma kerma coefficient comply well with the theoretical XCOM levels and experimental results at energies of 511, 661 and 1274 keV.

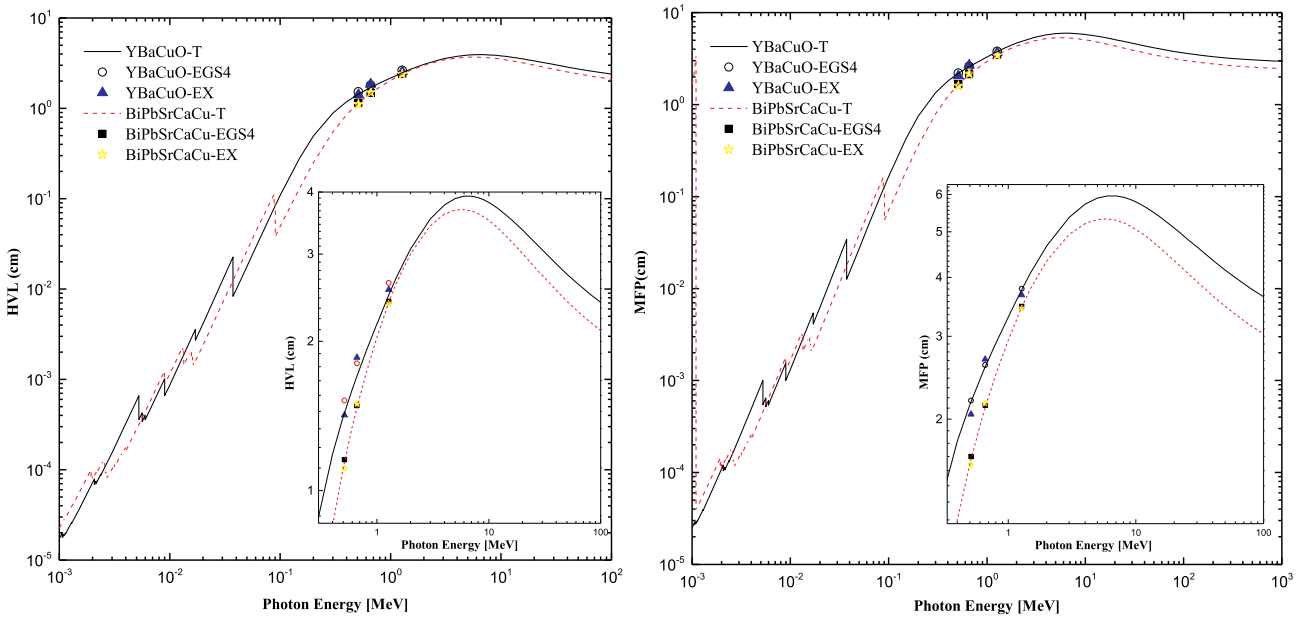

Fig. 2. Comparison of the half value layer and the mean free path for YBaCuO and BiPbSrCaCuO superconductors.

Table 4
Values of the theoretical (T and EGS4) and experimental (EX) kerma coefficients k (in pGy.cm^2/photon) for YBaCuO, BiPbSrCaCuO superconductors and several elements. The T values used in the present work are taken from the experimental values of μ/ρ reported by Baltaş et al. (2005).

Elements and compounds	k (in pGy.cm^2/photon)								
	511 keV			661 keV			1274 keV		
	T	EGS4	EX	T	EGS4	EX	T	EGS4	EX
^{8}O	2.43	2.47	2.41	3.11	3.12	3.10	5.43	5.44	5.38
^{20}Ca	2.47	2.44	2.49	3.14	3.10	3.19	5.43	5.41	5.58
^{29}Cu	2.40	2.40	2.39	2.97	2.93	2.96	5.01	4.99	5.06
^{38}Sr	2.59	2.54	2.61	3.03	2.99	3.05	4.86	4.84	4.95
^{39}Y	2.66	2.66	2.63	3.09	3.08	3.15	4.94	4.93	5.13
^{56}Ba	3.77	3.75	3.85	3.78	3.76	3.40	5.04	5.02	5.32
^{82}Pb	8.30	8.24	8.01	7.03	6.96	6.91	6.59	6.59	6.48
^{83}Bi	8.59	8.52	8.66	7.25	7.07	7.79	6.72	6.71	6.35
$YBa_2Cu_3O_7$	3.01	2.99	3.20	3.34	3.32	3.23	5.07	5.05	5.21
$Bi_{1.84}Pb_{0.}34Sr_{1.91}Ca2_{.03}Cu_{3.06}O_{10}$	5.08	5.02	5.23	4.84	4.79	4.75	5.79	5.77	5.83

It is observed that the gamma kerma coefficients in heavy atoms (high Z) are higher in the elements studied in Table 4. Fig. 4 also demonstrates the deviation in the gamma kerma coefficients for gamma ray energy and the atomic number of the six selected elements in an extended energy interval between 1 keV and 1000 MeV. Furthermore, Table 4 and Fig. 4 demonstrate the result of the analysis that the gamma kerma coefficients increase with increasing photon energy for O, Ca, Cu, Sr, Y and Ba atoms and decrease with increasing energy for Pb and Bi atoms at 511, 661 and 1274 keV. The scattering and absorption of gamma rays are associated with the atomic number of an element, and this is associated with composite materials' effective atomic number (Çevik and Baltas, 2007). It can be seen from Fig. 4 that the kerma coefficient curves for these elements shift towards a higher energy region with increasing atomic number. The alterations in the kerma coefficients dependent on energy may be attributed to the Z-dependence: the level of the mass attenuation coefficient in the photoelectric influence is relative to Z^{4-5}, while in the Compton area, it is relative to Z, and in the interval of higher energy, in which pair production is dominant, the mass attenuation coefficient differs as Z^2. Another reason may be that it depends soundly on the atomic number and the photon energy ($\sim Z^4/E^3$), and thus, a considerable diversity in kerma coefficients takes place, and greater kerma levels are obtained in heavy and intermediate atoms and low-energy gamma-rays (El-Khayatt, 2017). This may be clarified based on the dominant status of the processes of gamma ray interaction. For the low-energy region in which the photoelectric effect is dominant, the levels of the kerma coefficients increase due to increasing atomic number, and the electron acquires almost no kinetic energy in the interaction. This may be interpreted as that Compton scattering is almost elastic at low photon energies (Attix, 1986). The scattering and pair production processes dominate at higher energies, meaning that the value of the kerma coefficient is also higher.

The variation in this coefficient for superconductor compounds at the same photon energies is shown in Fig. 5. It may be observed in this figure that the kerma coefficients of BiPbSrCaCuO are higher than those of the YBaCuO superconductor sample for all energies (Fig. 5a). Since BiPbSrCaCuO has a higher effective atomic number than YBaCuO at 511, 661 and 1274 keV (Baltaş et al., 2005), it follows that there is a higher chance of interaction between the gamma rays and the material, giving a higher value of the kerma coefficient for materials with high effective atomic number (Kaur et al., 2019). In addition, the kerma coefficients increase for YBaCuO and decrease for BiPbSrCaCuO at 511, 661 and 1274 keV. This decrease can be attributed to the presence of Pb

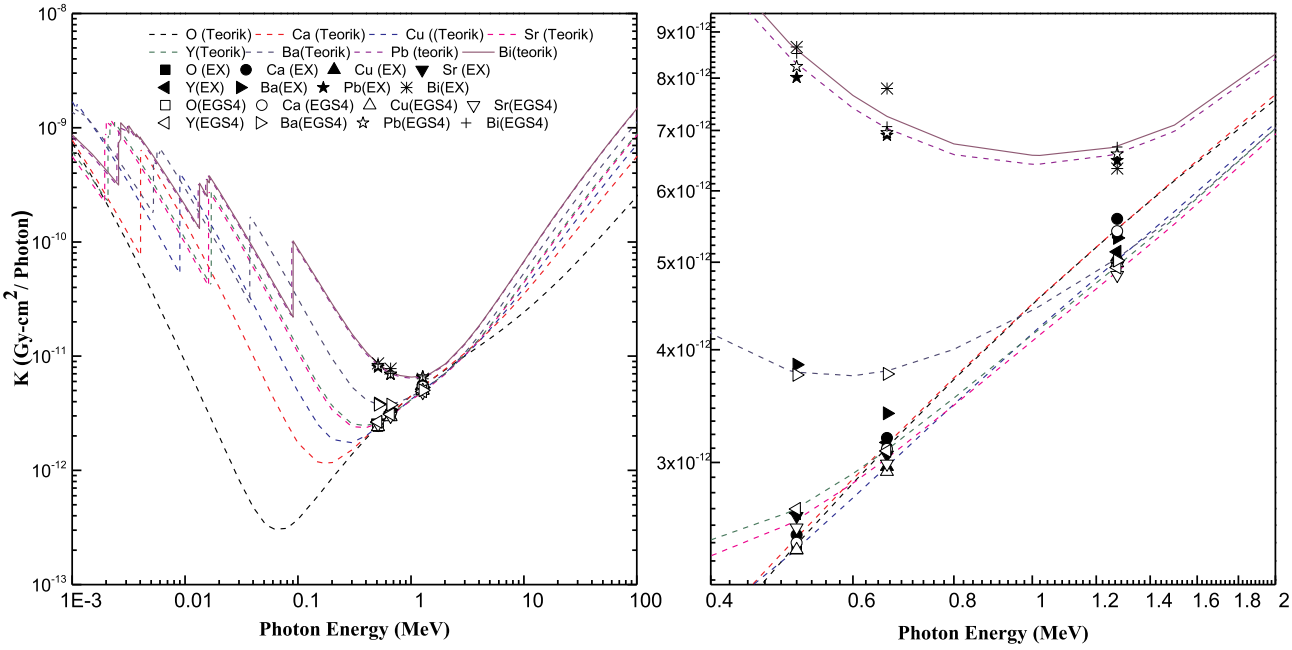

Fig. 4. Calculated theoretical (T, EGS4) and experimental (EX) gamma kerma coefficients for several elements as a function of photon energy: (a) for the full energy range, and (b) for an energy range close to that of the experimental data.

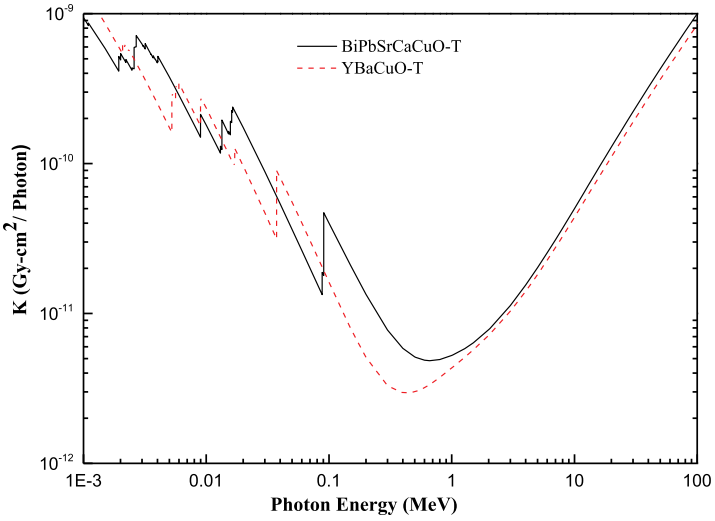

(a)

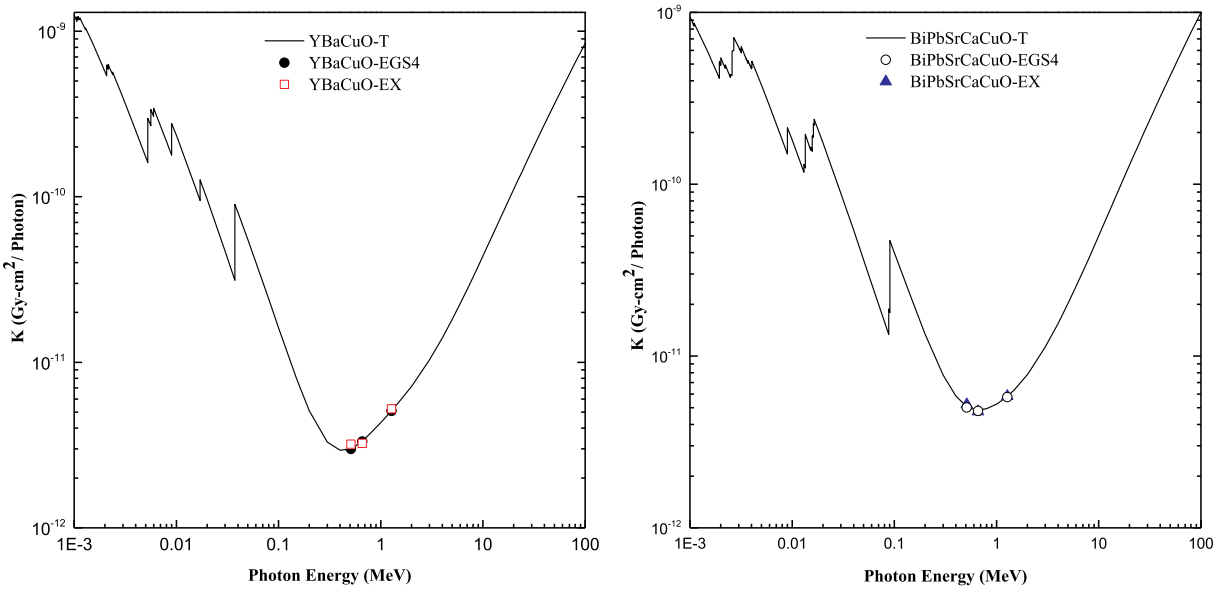

(b)

Fig. 5. Calculated theoretical (T, EGS4) and experimental (EX) gamma kerma coefficients for YBaCuO and BiPbSrCaCuO superconductor samples as a function of photon energy.

and Bi elements in the BiPbSrCaCuO superconductor. In the intermediate energy region, one may observe a reduction of the levels of the kerma coefficient with rising photon energy. Afterwards, the values of the kerma coefficient increase with increasing photon energy before a maximum value is obtained. One may see in Fig. 5b that the theoretical outcomes of the kerma coefficients display perfect compliance with the results from XCOM and the experimental values. As a result, the change in the gamma kerma coefficient follows the same trend in the investigated samples over the extended energy range.

4. Conclusion

In this study, the radiation attenuation parameters such as mass attenuation coefficient (μ/ρ), half value layer (HVL), mean free path (MFP), effective atomic number (Z_{eff}) and the gamma kerma coefficient (K) for YBaCuO and BiPbSrCaCuO superconductors and six elements were evaluated using the EGS4 code and XCOM software at gamma energies of 511, 661 and 1274 keV. The experimental data are found to be in agreement with the theoretical values calculated based on the XCOM program and the EGS4 simulation. The variation in the radiation attenuation parameters for the investigated samples was also computed in the different energies by utilizing the WinXCom program, and these are plotted. From the figures, it can be seen that all attenuation curves fit an identical trend, without regards to the type of material (El-Khayatt, 2017). The results showed that BiPbSrCaCuO sample is more effective than YBaCuO for gamma attenuation. This is may be due to Bi and Pb with higher atomic number in BiPbSrCaCuO sample. The present study will be useful in relation to the application of superconductivity in nuclear fusion reactors or accelerators.

Acknowledgment

I would like to thank Professor A.M. El-Khayatt of the Reactor Physics Department of, Nuclear Research Centre, Atomic Energy Authority, Professor L. Gerward of the Department of Physics, Technical University of Denmark for providing us with the experimental kerma formula and the WinXCom program, respectively. Also, I would like to thank Dr. Ahmet Celik of University of Giresun for his valuable support.

Appendix A. Supplementary data

Supplementary data to this article can be found online at https://doi.org/10.1016/j.radphyschem.2019.108517.

References

Abdel-Rahman, W., Podgorsak, E.B., 2010. Energy transfer and energy absorption in photon interactions with matter revisited: a step-by-step illustrated approach. Radiat. Phys. Chem. https://doi.org/10.1016/j.radphyschem.2010.01.007.

Attix, F.H., 1986. Introduction to Radiological Physics and Radiation Domisetry. John Wiley & Sons, U.S.A.

Ballarino, A., Shavkin, S.V., Bruchanov, A.N., Taylor, T.M., Kruglov, V.S., Ryazanov, P.V., Volkov, A.I., Latushkin, S.T., Lubimov, A.N., 2004. Effect of Fast Neutron Irradiation on Current Transport Properties of HTS Materials.

Baltaş, H., Çevik, U., Tirașoğlu, E., Ertuğral, B., Apaydm, G., Kobya, A.I., 2005. Mass attenuation coefficients of YBaCuO and BiPbSrCaCuO superconductors at 511, 661 and 1274keV energies. Radiat. Meas. 39, 33–37. https://doi.org/10.1016/j.radmeas.2004.01.005.

Baltaş, H., Çelik, Ş., Çevik, U., Yanmaz, E., 2007. Measurement of mass attenuation coefficients and effective atomic numbers for MgB2 superconductor using X-ray energies. Radiat. Meas. 42, 55–60. https://doi.org/10.1016/j.radmeas.2006.08.005.

Berger, M.J., Hubbell, J.H., 1987. XCOM: Photon cross sectionsdatabase, Web Version 1.2. Available Institute of Standards and Technology, Gaithersburg, MD 20899,USA. Originally published as NBSIR 87-3597, XCOM: Photon CrossSection on a Personal Computer.

Celik, N., Cevik, U., 2010. Monte Carlo determination of water concentration effect on gamma-ray detection efficiency in soil samples. Appl. Radiat. Isot. 68, 1150–1153.

Çelik, N., Özen, S.A., Demirtaş, Ö.F., Çevik, U., 2018. The effect of energy resolution of detection instrument on mass attenuation coefficient. J. Instrum. 13https://doi.org/10.1088/1748-0221/13/10/P10012. P10012–P10012.

Çevik, U., Baltaş, H., 2007. Measurement of the mass attenuation coefficients and electron densities for BiPbSrCaCuO superconductor at different energies. Nucl. Instrum. Methods Phys. Res. Sect. B Beam Interact. Mater. Atoms 256, 619–625. https://doi.org/10.1016/j.nimb.2007.01.131.

El-Khayatt, A.M., Vega-Carrillo, H.R., 2015. Photon and neutron kerma coefficients for polymer gel dosimeters. Nucl. Instruments Methods Phys. Res. Sect. A Accel. Spectrometers, Detect. Assoc. Equip. 792, 6–10. https://doi.org/10.1016/j.nima.2015.04.033.

El-Khayatt, A.M., 2017. Semi-empirical determination of gamma-ray kerma coefficients for materials of shielding and dosimetry from mass attenuation coefficients. Prog. Nucl. Energy 98, 277–284. https://doi.org/10.1016/j.pnucene.2017.04.006.

Gaikwad, D.K., Sayyed, M.I., Botewad, S.N., Obaid, S.S., Khattari, Z.Y., Gawai, U.P., Afaneh, F., Shirshat, M.D., Pawar, P.P., 2019. Physical, structural, optical investigation and shielding featuresof tungsten bismuth tellurite based glasses. J. Non-Cryst. Solids 503, 158–168.

Gasparro, J., Hult, M., Johnston, P.N., Tagziria, H., 2008. Monte Carlo modelling of germanium crystals that are tilted and have rounded front edges. Nucl. Instruments Methods Phys. Res. Sect. A Accel. Spectrometers, Detect. Assoc. Equip. 594, 196–201.

Gerward, L., Guilbert, N., Jensen, K.B., Levring, H., 2001. X-ray absorption in matter. Reengineering XCOM. Radiat. Phys. Chem. 60, 23–24.

Gerward, L., Guilbert, N., Jensen, K.B., Leving, H., 2004. WinXCom–a program for calculating X-ray attenuation coefficients. Radiat. Phys. Chem. 71, 653–654.

Kaur, T., Sharma, J., Singh, T., 2019. Review on scope of metallic alloys in gamma rays shield designing. Prog. Nucl. Energy 113, 95–113.

Kondo, K., Ochiai, K., Murata, I., Konno, C., 2008. Verification of KERMA factor for beryllium at neutron energy of 14.2 MeV based on charged-particle measurement. Fusion Eng. Des. 83, 1674–1677.

Krusin-Elbaum, L., Thompson, J.R., Wheeler, R., Marwick, A.D., Li, C., Patel, S., Shaw, D.T., Lisowski, P., Ullmann, J., 1994. Enhancement of persistent currents in Bi 2 Sr 2 CaCu 2 O 8 tapes with splayed columnar defects induced with 0.8 GeV protons. Appl. Phys. Lett. 64, 3331–3333. https://doi.org/10.1063/1.111269.

Kumar, A., Gaikwad, D.K., Obaid, S.S., Tekin, H.O., Agar, O., Sayyed, M.I., 2019. Experimental studies and Monte Carlo simulations on gamma ray shielding competence of (30 + x) PbO10WO3 10Na2O − 10MgO–(40-x) B2O3 glasses. Prog. Nucl. Energy 103047.

Luiz, A.M., 2011. Superconductivity-Theory and Applications.

Nelson, W.R., Rogers, D.W.O., Hirayama, H., 1985. The EGS4 Code System.

Obaid, S.S., Sayyed, M.I., Gaikwad, D.K., Pawar, P.P., 2018. Attenuation coefficients and exposure buildup factor of some rocks for gamma ray shielding applications. Radiat. Phys. Chem. 148, 86–94.

Olukotun, S.F., Gbenu, S.T., Ibitoye, F.I., Oladejo, O.F., Shittu, H.O., Fasasi, M.K., Balogun, F.A., 2018. Investigation of gamma radiation shielding capability of two clay materials. Nucl. Eng. Technol. 50, 957–962.

Petrean, A.M., Paulius, L.M., Kwok, W.K., Fendrich, J.A., Crabtree, G.W., 2000. Experimental evidence for the vortex glass phase in untwinned, proton irradiated YBa 2 Cu 3 O 7 − δ. Phys. Rev. Lett. 84, 5852–5855. https://doi.org/10.1103/PhysRevLett.84.5852.

Sawh, R.P., Weinstein, R., Ren, Y., Obot, V., Weber, H., 2000. Uranium fission fragment pinning centers in melt-textured YBCO. Phys. C Supercond. its Appl. 341–348 (I), 2441–2442. https://doi.org/10.1016/S0921-4534(00)01163-1.

Singh, V.P., Badiger, N.M., Vega-Carrillo, H.R., 2015. Neutron kerma coefficients of compounds for shielding and dosimetry. Ann. Nucl. Energy 75, 189–192.

Tekin, H.O., Singh, V.P., Manici, T., 2017. Effects of micro-sized and nano-sized WO 3 on mass attenuation coefficients of concrete by using MCNPX code. Appl. Radiat. Isot. 121, 122–125. https://doi.org/10.1016/j.apradiso.2016.12.040.

Tekin, H.O., Altunsoy, E.E., Kavaz, E., Sayyed, M.I., Agar, O., Kamislioglu, M., 2019. Photon and neutron shielding performance of boron phosphate glasses for diagnostic radiology facilities. Results Phys 12, 1457–1464.

Thomas, D.J., 2012. ICRU Report 85: Fundamental Quantities and Units for Ionizing Radiation.

Turner, J.E., 2008. Atoms, Radiation, and Radiation Protection. John Wiley & Sons.

Ueda, H., Ishiyama, A., Miyahara, N., Kashima, N., Nagaya, S., 2009. Radioactivity of YBCO and Bi-2223 tapes under low energy neutron flux. IEEE Trans. Appl. Supercond. 19, 2872–2876.

Yamaguchi, I., Ohba, H., 2014. Monte Carlo calculation of external dose rate around a radionuclide reservoir tank using EGS4. Radiat. Saf. Manag. 2, 29–32. https://doi.org/10.12950/rsm2002.2.29.

Zhang, L., Abdou, M.A., 1997. Kerma factor evaluation and its application in nuclear heating experiment analysis. Fusion Eng. Des. 36, 479–503.